MedCrave
Step into the World of Research

Aeronautics and Aerospace Open Access Journal

Research Article

Open Access

CrossMark

Active injection method for fluidic winglet

Abstract

Various solutions for the fluidic winglet are proposed to investigate the impact of parameters such as velocity, temperature and injection direction, and slot area for air ejection. This study is based on the replacement to A380 solid winglet. The results reveal that maximising these parameters doesn't always minimise drag; rather, a balance needs to be found to achieve optimal efficiency. The study demonstrates a potential maximum reduction of 3.81%, often linked with a decrease in lift. The optimal design is a single rectangular slot injecting at 260 m/s, exhibiting lower lift reduction than drag reduction and high efficiency. Thus, currently, there isn't a significant advantage justifying a paradigm shift for these devices.

Keywords: computational fluid dynamics, aircraft performance, clean wing, winglet, fluidic winglet, wingtip vortices

Volume 8 Issue 1 - 2024

Amir Zare Shahneha
Cranfield University, United Kingdom

Correspondence: Amir Zare Shahneha, Centre of Aeronautics, Cranfield University, Cranfield, MK43 0AL, United Kingdom, Email a.shahne@cranfield.ac.uk

Received: February 12, 2024 | **Published:** March 01, 2024

Introduction

Air transportation has been grown up by 3.6% from 2019 to 2041, recovering to pre-pandemic levels by 2023.[1] This increased demand for aircraft coincides with a growing awareness of emissions in the aeronautical industry, leading to extensive research by manufacturers to develop cleaner vehicles.

To tackle emissions, winglets have been introduced to reduce drag and emissions by mitigating the vortex effect's thrust requirements. However, these winglets are effective mainly at low-speed flight, adding weight and parasite drag.

The objectives include studying an alternative approach to reduce wingtip vortices without structural changes. The project involves examining winglet structures, optimising fluidic winglet design through lift and drag coefficient analysis, and evaluating the chosen design's performance during the cruise phase. The process comprises steps like theory review, preliminary investigation, geometry modeling, and CFD simulations using CATIA and ANSYS Fluent software.

Fluidic Winglet

Theory behind wingtip vortices is explained here and the current solutions to reduce their impact will be discussed. It also covers the selection of wing and structural winglet geometries and introduces proposed fluidic winglet slots. A basic design proposal for the fluidic winglet architecture is included.

Wingtip vortices

Aircraft flight relies on lift generated by pressure differences between wing surfaces as air flows at varying speeds. However, at wingtips, air circulates in vortices, creating induced drag. This drag can be reduced using wingtip devices to increase effective wingspan and minimise vortices.

The vortex's position relative to the wing affects wingspan, impacting lift and drag. Increasing span reduces induced drag. Initial winglets, resembling wingtip fences, prevent air recirculation, eliminating the need for higher angles of attack. Modified winglets, with a wing-like shape and tilt, further reduce induced drag and enhance lift, aiding vortex reduction. Studies have explored aircraft fluidic winglets at Mach 0.3, with elongated slots proving most effective.[2]

Wing geometry selection

The A380-800, known for its high passenger capacity and long-range capabilities, is chosen as the base model for the study of wing geometry. This wide-body aircraft with four engines has a cruise Mach speed of 0.82 and a cruising altitude of 10,670 meters. While the A380 underwent fewer changes from its original version, one notable modification is the introduction of more efficient "downlet" winglets, which reduce fuel consumption by 4% compared to the original "winglet fence" design.[3]

The study uses the A380's "clean wing" (without winglets) as the base wing configuration. The winglet model chosen for analysis is the commonly used "winglet fence". Geometry parameters for both the clean wing and winglets are obtained from the manufacturer document.[4] The clean wing geometry parameters shows the values of root chord, kink chord and tip chord dimensions when there is no winglet. The span size, sweep angle and dihedral angle for the chosen aircraft are stated in Table 1. The wing profile used is a supercritical one, approximated using the NASA SC(2)-0610 model for the wing root.[5]

Design of fluidic winglet

Different fluidic winglet slot geometries have been tested, including a single rectangular slot on the wingtip's lateral surface, which can be evolved by adding another rectangular slot to the upper surface. This modification increases the area and changes the flow direction. The parameters for these configurations are detailed in Table 2, and their models can be seen in Figure 1.

Another configuration comprises 10 circular slots with a diameter equal to the height of the rectangular slot, evenly spaced to occupy the same length as the rectangle. The diameter can be adjusted, as explained later. Parameters for this configuration are provided in Table 3.

Fluidic winglet architecture

Fluidic winglet architecture is shown in Figure 1. The top-level conceptual design of the air supply system is presented without detail design. It explores different sources for obtaining air, proposing the use of aircraft engines. The airflow passes through a pressure regulator valve, a shut-off valve, and potentially a heat exchanger before reaching a distributor that feeds it into the wingtip slots.

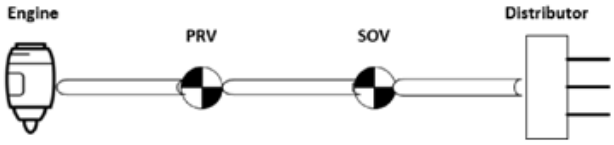

Figure 1 Fluidic winglet system architecture.

Table 1 Clean wing geometry parameters

Parameter	Value
Root chord	17.67 m
Kink chord	13.75 m
Tip chord	3.98 m
Semi-span	39.88 m
Sweep angle	35.44°
Dihedral angle	5.36°

Table 2 Rectangular slot parameters

Parameter	Value	
Height	2%	chord
Width	54%	chord
Distance from the leading edge	15%	chord
Distance from the wing tip (for the 2 slot configuration)	3%	chord

Table 3 Circular slot parameters

Parameter	Value
Diameter	2% chord
Distance from the leading edge	15% chord
Slot separation	3.8% chord

Methodology

This section outlines the methodology for modelling various proposed solutions and reference cases, along with the processes for mesh generation and preparing Computational Fluid Dynamics (CFD) simulations to acquire the aerodynamic characteristics of the A380 wing.

Geometry modelling

The wing's geometry is established using CATIA V5, modelling only half of the wing due to symmetry, Figure 2. This model is then imported into ANSYS Workbench for domain generation and subsequent meshing. The computational domain is symmetrical about the horizontal plane and covers a rectangular area measuring 176.7 m in length and 35.34 m in height. It includes a semicircle originating from the leading edge with a radius of 176.7 m, allowing for angle of attack adjustments without the need for new models. The extension of 10 times the root chord in all directions and applied boundary conditions ensure accurate physics modelling without compressibility effects. Figure 3 shows the CAD models for the different geometries of the fluidic winglets.

Mesh modelling

The ANSYS software is used for meshing the fluid domain, employing a mesh generation algorithm that starts with a surface mesh and then creates a volumetric mesh, Figure 4. The mesh is refined in areas of interest, including the wing surfaces and boundary layers. Specific characteristic dimensions are set for different elements, such as 0.07 m for upper and lower wing surfaces and 0.03 m for leading edges, trailing edges, and the wingtip. Inflation controls consist of 22 layers with specific height and growth ratios. Minimum and maximum element dimensions for the rest of the domain are set at 0.01 and 5 m, respectively, with a growth ratio of 20%.

Figure 2 Clean wing model.

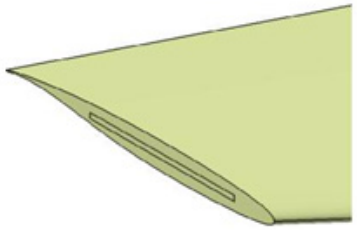

(a) Single rectangular configuration.

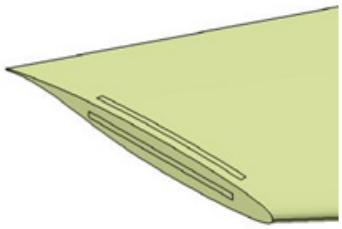

(b) Two rectangular slots Fluidic configuration.

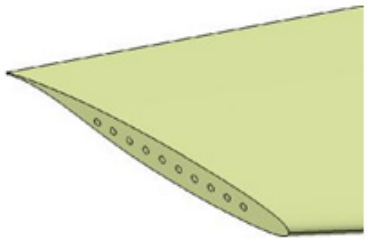

(c) Circular slots fluidic configuration.

Figure 3 CAD models for the different geometries of the fluidic winglets.

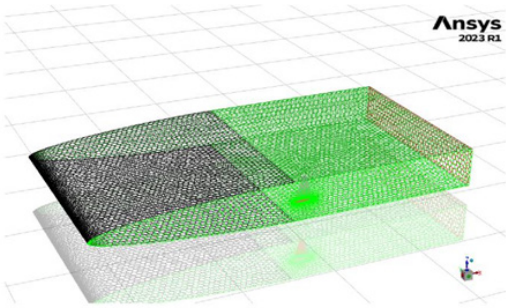

Figure 4 Mesh for the fluidic domain and wing geometry.

All these parameters result in a total of 7,229,987 polyhedral elements, with a higher concentration near the surface due to the imposed inflation, which faithfully simulates the phenomena related to wall friction in a realistic manner.

Boundary conditions

The simulation employs a steady-state, pressure-based solver considering gravity. Boundary conditions are set with pressure-far-field boundaries for the upper, lower, and lateral walls, symmetry for the wing-contacted side, and pressure-far-field for curved inflow and rear outflow. Wing and winglet walls are defined as solid, fluidic winglet slots as velocity inlets. Operational conditions include pressure, temperature, air as the medium, density using the ideal gas law, and viscosity via Sutherland's law. Cruise Mach number is 0.82, with velocity vector direction adjusted for angle of attack. The energy equation and realisable k-epsilon turbulence model govern the fluid domain.

Results and analysis

This section provides the parameters derived from CFD simulations for comparative aerodynamic analysis of each proposed scenario. This analysis aims to identify the optimal choice among them and evaluate its feasibility by comparing it with the existing solution.

Clean wing

Table 4 the values of aerodynamic coefficients for the clean wing at cruise conditions are tabulated. Figure 5 shows the outcome of CFD simulations for the clean wing under various cruising conditions at angles of attack ranging from 0 to 10 degrees, which the contours are shown in Figure 6. These angles cover a representative range for the cruise phase. It is important to note that the aerodynamic forces are expressed in wind axes, which vary with the angle of attack. The lift and drag coefficients for the reference cases show a linear increase with the angle of attack, as expected. Additionally, the simulations reveal the formation of an oblique shock wave near the wing's leading edge, with higher angles of attack resulting in a greater velocity vector inclination. At a 10-degree angle of attack, the velocity angle causes less change before the oblique shock. However, the presence of this shock wave at 6.25 degrees leads to significant velocity and pressure differences.

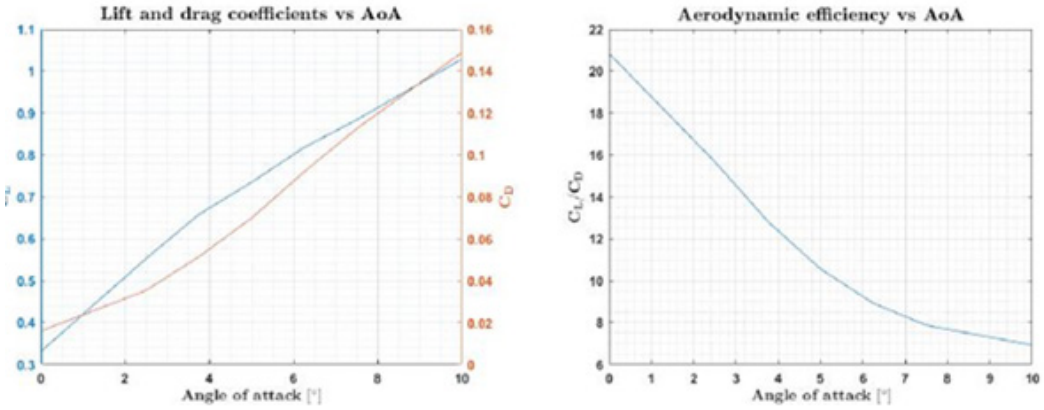

Figure 5 Aerodynamic coefficients for the clean wing in cruise conditions.

(a) Lift and drag coefficients for the clean wing.

(b) Aerodynamic efficiency for the clean wing.

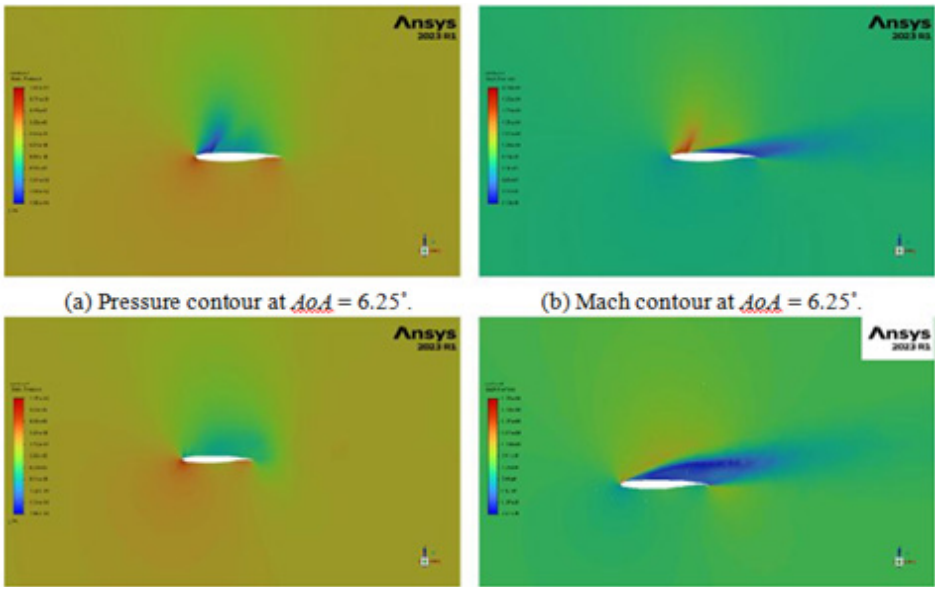

Figure 6 Pressure and Mach contours for the clean wing at different angles of attack.

Table 4 Aerodynamic coefficients for the clean wing at cruise conditions

AoA [°]	CL	CD	CL/CD
0	0.3309	0.0151	21.9128
2.5	0.5526	0.0384	14.3897
3.75	0.6573	0.0559	11.759
5	0.7341	0.0766	9.5833
6.25	0.8172	0.0932	8.7686
7.5	0.8831	0.1124	7.8568
10	1.0281	0.1487	6.9134

Wing with structural winglet

Table 5 shows the percentage difference in the aerodynamic coefficients between the structural winglet and the clean wing in cruise conditions. Fluent has been used to simulate the actual winglet model installed on the clean wing which resulted to a consistent trend similar to the clean wing, with both lift and drag coefficients following a linear progression as the angle of attack changes, as seen in Figure 7. The winglet introduces a reduction in drag and an increase in lift, leading to a substantial improvement in aerodynamic efficiency. The reduction in drag coefficient is more pronounced at lower angles of attack and diminishes at higher angles. On average, these variations range from 4 to 5 percent for angles representative of the cruise phase. Aerodynamic efficiency is notably higher when the wing is positioned more horizontally. At 0 degrees angle of attack, efficiency is approximately 8 times greater than at 10 degrees. The figure also reveals that aerodynamic efficiency decreases parabolically with the angle of attack.

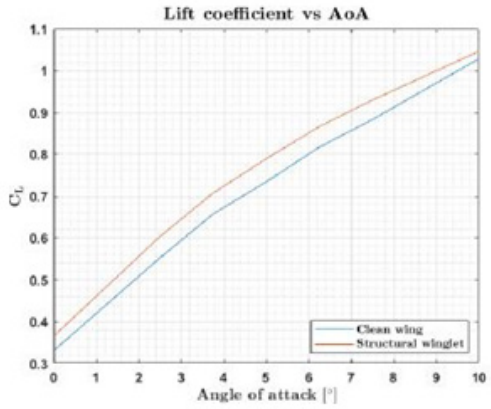

a. Lift coefficients for the clean wing and structural winglet.

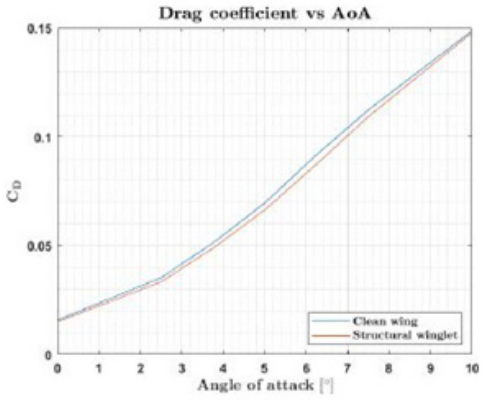

b. Drag coefficients for the clean wing and structural winglet.

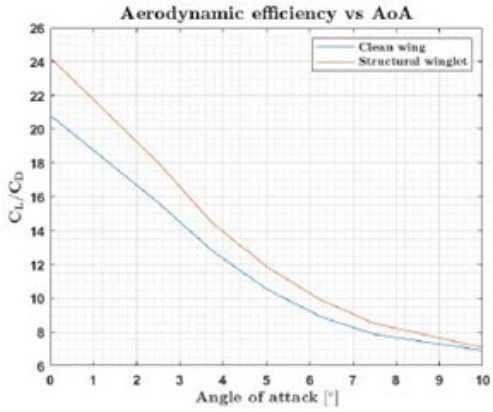

c. Aerodynamic efficiency for the clean wing and structural winglet.

Figure 7 Aerodynamic coefficients for the clean wing and structural winglet in cruise conditions.

Table 5 Percentage difference in the aerodynamic coefficients between the structural winglet and the clean wing in cruise conditions

AoA [°]	LCL (%)	LCD (%)	LCL/CD (%)
0	10.4216	-5.1255	16.387
2.5	9.2401	-5.0849	15.0924
3.75	7.6289	-4.6901	12.9252
5	7.5248	-4.5203	12.6154
6.25	6.0034	-4.6594	11.1839
7.5	5.2671	-2.6968	8.1846
10	1.7401	-0.5842	2.338

Wing with fluidic winglet

The study proceeds by simulating various proposals for the implementation of the fluidic winglet, aiming to identify the most optimal solution. Different configurations involving varying injection velocity, temperature, injection angle, and slot parameters are tested. The concept behind modifying these parameters is based on the jet momentum coefficient, which is a product of flight conditions and a form factor. This form factor represents the slot area to wing surface area ratio, while the first component involves the injection velocity relative to the free-stream velocity.

Injection velocity

The initial analysis examines the impact of injection velocity, with flight and sound velocities as reference points. The goal is to maximise the ratio of injection velocity to free stream velocity, enhancing the jet momentum coefficient. Simulations are conducted in the range of 250 to 290 m/s with 10 m/s intervals. Two geometries are used: one with a single rectangular slot at the wingtip and another with 10 circular slots matching the dimensions of the rectangular slot, evenly spaced to match its length.

Rectangular slot

In the case of the rectangular slot, all lift coefficients are around 0.8, with higher values for the proposed minimum and maximum injection velocities, peaking at 270 m/s. This trend is reflected in aerodynamic drag as well. Compared to the clean wing, all velocities result in reduced drag coefficients, but they are higher than when using structural winglets. It is important to note that lift production is reduced to varying degrees across all cases.

Aerodynamic efficiency values also decrease across all cases. However, 260 and 290 m/s velocities show positive efficiency values compared to the clean wing. Despite representing the second-highest drag reduction, 260 m/s results in significantly smaller percentage losses in lift compared to the maximum reduction case.

Table 6 presents the percentage difference in the aerodynamic coefficients between the rectangular slot configuration and the structural winglet and the clean wing in cruise conditions. Figure 8 illustrates the trajectory of air particles exiting the slot, showing an immediate curvature due to the interaction with the wingtip vortex.

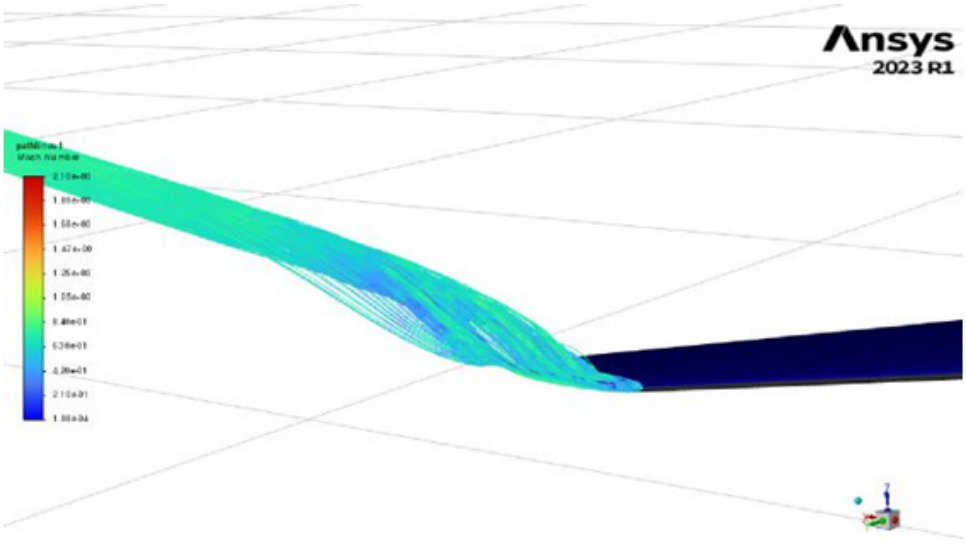

Figure 8 Streamlines for the injection flow for the rectangular slot.

Table 6 Percentage difference in the aerodynamic coefficients between the rectangular slot configuration and the structural winglet and the clean wing in cruise conditions

VJ [m/s]	Clean wing			Structural winglet		
	ΔCL (%)	ΔCD (%)	ΔCL/CD (%)	ΔCL (%)	ΔCD (%)	ΔCL/CD (%)
250	-1.975	-0.9908	-0.994	-7.5265	3.8479	-10.9529
260	-2.5182	-2.7155	0.2028	-8.039	2.0389	-9.8765
270	-6.358	-2.8065	-3.654	-11.6613	1.9434	-13.3454
280	-2.9925	-0.2188	-2.7798	-8.4865	4.6576	-12.5591
290	-0.4761	-0.4807	0.0046	-6.1126	4.383	-10.0548

Round slots

The geometry with circular slots follows a similar trend. Aerodynamic coefficients reach a minimum at 270 m/s, but they are higher than those for the rectangular slot. Aerodynamic efficiencies are also higher for circular slots, but the choice between efficiency and drag reduction depends on comparisons with reference cases. Table 7 shows the percentage difference in the aerodynamic coefficients between the round slots configuration and the structural winglet and the clean wing in cruise conditions.

Table 7 Percentage difference in the aerodynamic coefficients between the round slots configuration and the structural winglet and the clean wing in cruise conditions

VJ [m/s]	Clean wing			Structural winglet		
	ΔCL (%)	ΔCD (%)	ΔCL/CD (%)	ΔCL (%)	ΔCD (%)	ΔCL/CD (%)
250	-0.5061	-0.6469	0.1417	-6.1409	4.2086	-9.9315
260	-0.7646	-0.1877	-0.578	-6.3847	4.6903	-10.5788
270	-4.7893	-2.0357	-2.8108	-10.1814	2.7519	-12.587
280	-1.8536	-1.1377	-0.7242	-7.412	3.6938	-10.7103
290	-2.6642	-0.1453	-2.5226	-8.1767	4.7347	-12.3277

In the case of circular slots, the largest reduction compared to the clean wing is again observed at 270 m/s, but in this instance, the losses in lift are twice as much. When compared to structural winglets, it is evident that the losses in lift are smaller, yet drag is higher in all cases, narrowing the gap in efficiency.

This configuration also exhibits a clockwise circulation, though to a lesser extent, due to the presence of the vortex. Figure 9 shows the streamlines for the injection flow for the circular slot.

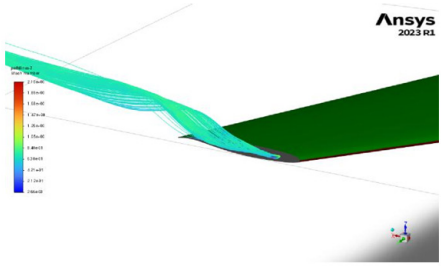

Figure 9 Streamlines for the injection flow for the circular slot.

Temperature of injection

The effect of varying air temperature on fluidic winglet performance has been investigated, with temperatures ranging from ambient temperature at cruise altitude up to 300K, including 250K and 270K. In Table 8 the percentage difference in the aerodynamic coefficients between the rectangular slot configuration with different injection temperatures and the reference cases in cruise conditions are presented. These temperatures are selected based on estimates of the secondary flow temperature from the engine.

Table 8 Percentage difference in the aerodynamic coefficients between the rectangular slot configuration with different injection temperatures and the reference cases in cruise conditions

TJ [K]	Clean wing			Structural winglet		
	ΔCL (%)	ΔCD (%)	ΔCL/CD (%)	ΔCL (%)	ΔCD (%)	ΔCL/CD (%)
218.795	-2.5182	-2.7155	0.2028	-8.039	2.0389	-9.8765
250	0.0599	-0.8439	0.9115	-5.6069	4.002	-9.2391
270	-2.9118	-1.1552	-1.7771	-8.4103	3.6754	-11.6572
300	-4.0287	-0.5947	-3.4546	-9.4639	4.2634	-13.166

The simulations show that the lowest drag coefficient occurs at ambient temperature, deteriorating as the gas is heated. This trend is inversely pro-portional to the injection Mach number, with the minimum drag coefficient occurring at the highest injection Mach number.

The highest percentage reduction in drag is observed at 218.795K, derived from the velocity study. However, as the temperature increases, losses in lift become significantly greater, reaching up to 8 times those of drag at 300K. Notably, the scenario involving a temperature of 250K shows a drag reduction of less than 1% and no losses in lift, resulting in an efficiency increase of 0.91%.

Slot area

Modifying the slot geometry to maximise the jet momentum coefficient by increasing the slot area is explored. For the circular slot model, the diameter of each of the 10 slots is increased up to 4% of the tip chord. This adjustment does not alter the trend of the aerodynamic coefficients, which exhibits a minimum at 270 m/s and increases as simulations diverge from this injection velocity. Efficiencies show subtle improvements, but their mean remains relatively stable at around 8.7. The lift coefficient also increases but maintains a mean value within the same range.

Increasing the slot area results in a greater reduction in drag relative to the clean wing, with lift coefficients generally showing a slight increase. This leads to a positive efficiency for the velocity with the lowest drag coefficient.

Rectangular slot

For the rectangular configuration, adjusting the efflux angle leads to the lowest drag coefficient, while only increasing the sweep angle results in a coefficient higher than normal flow. Combining both angle modifications yields the best efficiency but also the most significant reduction in lift, which is counterproductive.

In the case of two rectangular slots, it is similar to altering the injection angles, with the minimum drag coefficient occurring at 270 m/s. The efficiency is 8.6696, and there is a 3.81% drag reduction. The presence of two slots allows for more effective vortex translation due to the generation of two recirculation.

Conclusion

According to Table 9, A380 operating parameters, the analysis of A380 wing airflow has been conducted, Table 10, considering various angles of attack and configurations, including a clean wing and a winglet fence.

Table 9 A380 operating parameters

Parameter	Value
Wing area	845 m^2
MTOW	560000 kg
Cruise altitude	10670 m
Cruise speed	243.1546 m/s
Thurst	348 kN
Range	14816 km

Source: Jane's Group UK Limited.[3]

Table 10 Performance analysis results

Parameter	Value
Emax	7.9113
Vmd	228.0108 m/s
ui	1.0664
sfc	2.6940 · 10−6 kg/Ns
ω	1.2832
Range	17545.8308 km

The study explores the potential of replacing structural winglets with fluidic ones by varying parameters like injection velocity, direction, temperature, slot area, and shape.

The efficiency of fluidic winglets relies on careful control of injection parameters. Maximising all variables for high jet momentum coefficient is not the best approach. Moving the vortex farther by increasing dihedral angle reduces drag, but raising the sweep angle alone does not yield the expected improvement.

Doubling the slot area does not double drag reduction; increased injected flow diminishes efficiency. Aerodynamic efficiency improves only for angles below 6.25◦ despite greater drag reduction at higher

angles. The optimal fluidic winglet configuration combines substantial drag reduction with a minor lift decrease, achieving a 2.72% reduction and curbing lift losses to 2.52% at an angle of attack of 6.25◦. These are shown in Figure 10.

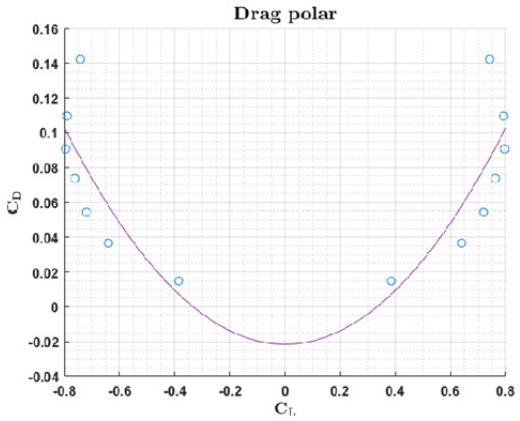

Figure 10 Drag polar for the fluidic winglet configuration.

Despite these findings, local stall potential and the traditional winglet's superiority at specific angles of attack justify maintaining the existing wingtip devices.

Acknowledgments

I highly appreciate my colleague Mr Rubio who motivated and engaged in the results.

Conflicts of interest

The authors declare that there is no conflict of interest.

References

1. Shparberg S, Lange B. Global market forecast 2022. 2022.
2. Mineck RE. Study of potential aerodynamic benefits from span wise blowing at wing-tip. Hampton, Virginia: Langley Research Center; 1995.
3. Jane's Group UK Limited, Airbus A380, 2023.
4. A380 aircraft characteristics airport and maintenance planning. Airbus SAS Blagnac; 2020.
5. Harris CD. NASA supercritical airfoils, Hampton, Virginia; 1990.